Study on Morphology of Ternary Polymer Blends. I. Effects of Melt Viscosity and Interfacial Interaction

M. HEMMATI,[1,2] H. NAZOKDAST,[1] H. SHARIAT PANAHI[1,2]

[1] Department of Polymer Engineering, Amir Kabir University, P.O. Box No.15875-4413 Tehran, Iran

[2] Department of Polymer Science and Technology, Research Institute of Petroleum Industry, P.O. Box No.18745-4163 Tehran, Iran

Received 21 July 2000; accepted 2 December 2000

ABSTRACT: The morphology of some ternary blends was investigated. In all of the blends polypropylene, as the major phase, was blended with two different minor phases, ethylene–propylene–diene terpolymer (EPDM) or ethylene–propylene–rubber (EPR) as the first minor phase and high-density polyethylene (HDPE) or polystyrene (PS) as the second minor phase. All the blends were investigated in a constant composition of 70/15/15 wt %. Theoretical models predict that the dispersed phase of a multiphase polymer blend will either form an encapsulation-type phase morphology or phases will remain separately dispersed, depending on which morphology has the lower free energy or positive spreading coefficient. Interfacial interaction between phases was found to play a significant role in determining the type of morphology of these blend systems. A core–shell-type morphology for HDPE encapsulated by rubber was obtained for PP/rubber/PE ternary blends, whereas PP/rubber/PS blends showed a separately dispersed type of morphology. These results were found to be in good agreement with the theoretical predictions. Steady-state torque for each component was used to study the effect of melt viscosity ratio on the morphology of the blends. It was found that the torque ratios affect only the size of the dispersed phases and have no appreciable influence on the type of morphology. © 2001 John Wiley & Sons, Inc. J Appl Polym Sci 82: 1129–1137, 2001

Key words: melt viscosity; interfacial interaction; morphology; ternary polymer blends

INTRODUCTION

Blending of immiscible polymers is widely applied as a versatile method to tailor materials for specific applications.[1–3] To date developments of polymer blends have been mainly focused on two-component systems. These systems are generally composed of a major and minor phase, of which the major component forms the matrix in which the minor phase disperses. Morphology of such systems is determined by blending history,[4,5] composition,[6,7] interfacial tension,[7–9] and viscosity ratio[6,8] of the disperse phase to matrix. In the pursuit of obtaining new polymeric blend materials, attention has been drawn to systems having more than two phases.[10–14] For ternary systems there are multiple types of phase morphology available that directly influence the whole set of properties.[10,14–16]

Correspondence to: H. Nazokdast.

Journal of Applied Polymer Science, Vol. 82, 1129–1137 (2001)

Table I Properties and Producers of Polymers Used

Polymer	Density (g/cm^3)	T_m (°C)	MFI (g/10 min)	Mooney Viscosity ML(1 + 4), 125°C	C_2 Content (%)	ENB Content (%)	Producer
HDPE1	0.964	130	0.35[a]	—	—	—	5200 B, Iran Petrochemical
HDPE2	0.952	126	14[a]	—	—	—	HD5218EA, Iran Petrochemical
PP	0.9	165	0.27[b]	—	—	—	MOPLEN 60R, Iran Petrochemical
EPDM1	0.86	—	—	30	50	5	Buna AP241, Bayer Co.
EPDM2	0.87	—	—	61	70	5	Buna AP447, Bayer Co.
EPR	0.86	—	—	35	75	—	Vistalon 805, Exxon Chemical
PS	1.05	185	1.6[c]	—	—	—	1070, Iran Petrochemical

[a] 190°C/2.160 kg.
[b] 230°C/2.160 kg.
[c] 200°C/5 kg.

For ternary systems containing two minor phases dispersed in a continuous matrix, three distinct types of phase morphology were considered. Hobbs et al.[17] reported one minor component encapsulating another with a core–shell morphology for some systems, whereas in other systems two minor components disperse separately in a matrix. Luzinov et al.[14] suggested a third situation, which is an intermediate case, in which mixed phases of two minor components are formed without any ordered organization.

Because the mechanical properties and rheology of ternary systems are greatly influenced by their phase morphologies,[10,11,14–16] it is important to understand the factors affecting the phase structures of multicomponent systems to predict and control the phase morphology. Viscosity of components, composition, interfacial interaction between phases, and processing parameters are found to be the main factors that influence morphology of ternary polymer blends.[12,14,17]

In the present work the effects of viscosity and interfacial interaction of components on morphology of ternary polymer blends were investigated. Theoretical concepts were used to predict the morphology of some ternary polymer blends of PP, PE, PS, EPDM, and EPR.

Table II Nomenclature and Components of Blends

Sample	Major Phase	Minor Phase (1)	Minor Phase (2)
1	PP	EPDM1	HDPE1
2	PP	EPDM2	HDPE1
3	PP	EPDM1	HDPE2
4	PP	EPDM2	HDPE2
5	PP	EPR	HDPE1
6	PP	EPR	HDPE2
7	PP	EPDM1	PS
8	PP	EPDM2	PS
9	PP	EPR	PS

Table III Estimated Surface Tension of Polymers at the Mixing Temperature (190°C)

Polymer	γ (190°C) (mN/m)	γ_p (190°C) (mN/m)	γ_d (190°C) (mN/m)
PP	20.22	0.4	19.81
HDPE[a]	25.93	0	25.93
PS	28.48	4.78	23.7
EPDM1	23.15	0.21	22.94
EPDM2	24.3	0.13	24.17
EPR	24.5	0.1	24.4

[a] Interfacial tensions of HDPE1 and HDPE2 are assumed to be the same.

Table IV Estimated Interfacial Tensions at 190°C

Interface	Interfacial Tension at 190°C (dyn cm^{-1})
PP/PE	1.23
PP/EPDM1	0.32
PP/EPDM2	0.63
PE/EPDM1	0.39
PE/EPDM2	0.19
PP/PS	4.06
PS/EPDM1	4.19
PS/EPDM2	4.41
PP/EPR	0.67
PE/EPR	0.14
PS/EPR	4.49
PE/PS	4.88

Interfacial Interaction Effect

Hobbs et al.[17] and Luzinov et al.[14] used Harkin's[18] spreading coefficient concept to explain the effect of interfacial tension between phases on the phase morphology of different ternary blends. For a ternary system with A as the continuous phase and B and C as the dispersed phases the spreading coefficient λ_{BC} of the B-phase on the C-phase[18] is

$$\lambda_{BC} = \gamma_{AC} - \gamma_{AB} - \gamma_{BC} \quad (1)$$

where γ_{AC}, γ_{AB}, and γ_{BC} are the interfacial tension for each component pair. If λ_{BC} is positive, the B-phase will encapsulate the C-phase. Similar treatment gives the spreading coefficient of the C-phase on the B-phase:

$$\lambda_{CB} = \gamma_{AB} - \gamma_{AC} - \gamma_{BC} \quad (2)$$

A positive value of λ will lead to a core–shell morphology in which the C-phase will encapsulate the B-phase. If both λ_{BC} and λ_{CB} are negative, the B and C phases will remain separate.

Guo et al.[12] reported that the equilibrium phase structure of a multiphase system is determined not by interfacial tension alone, but rather by the interfacial free energy that presents a combination of interfacial tension and interfacial areas. These authors introduced three equations to calculate the interfacial free energies of ternary systems with different phase structures:

$$\left(\sum A_i\gamma_{ij}\right)_{B+C} = (4\pi)^{1/3}[n_B^{1/3}x^{2/3}\gamma_{AB} + n_C^{1/3}\gamma_{AC}] \times (3V_C)^{2/3} \quad (3)$$

$$\left(\sum A_i\gamma_{ij}\right)_{B/C} = (4\pi)^{1/3}[n_B^{1/3}(1+x)^{2/3}\gamma_{AB} + n_C^{1/3}\gamma_{BC}] \times (3V_C)^{2/3} \quad (4)$$

$$\left(\sum A_i\gamma_{ij}\right)_{C/B} = (4\pi)^{1/3}[n_B^{1/3}x^{2/3}\gamma_{BC} + n_C^{1/3}(1+x)^{2/3}\gamma_{AC}](3V_C)^{2/3} \quad (5)$$

where A_i is the interfacial area of each phase in the system, $x = V_B/V_C$, V_i is the volume of each phase, and n_B and n_C are the numbers of particles in the B and C phases in the system, respectively. They assumed that $n_B = n_C$ and calculated the interfacial energy for each phase structure. The dominant phase morphology is the one with the

Table V Calculated Spreading Coefficients and Relative Interfacial Energies at 190°C (Samples 1 to 6)

	Blend Components			RIE				
Sample	A	B	C	B/C	C/B	B + C	λ_{CB}	λ_{BC}
1 and 3	PP	EPDM1	HDPE1 or HDPE2	0.9	2.34	1.55	−1.3	0.52
2 and 4	PP	EPDM2	HDPE1 or HDPE2	1.19	2.14	1.86	−0.79	0.41
5 and 6	PP	EPR	HDPE1 or HDPE2	1.2	2.09	1.9	−0.7	0.42

Table VI Steady-State Torque of Polymers at 190°C and 60 rpm

Polymer	Steady-State Torque at 190°C/60 rpm (Nm)
PP	17
HDPE1	19.2
HDPE2	0.5
EPDM1	16.5
EPDM2	41.2
EPR	15.3
PS	32.8

lowest interfacial energy. The assumption made by Guo et al.[12] was used in the present work to simplify eqs. (3)–(5) into the following equations:

$$(\mathrm{RIE})_{B+C} = \left(\sum A_i \gamma_{ij}\right)_{B+C} /K = x^{2/3}\gamma_{AB} + \gamma_{AC} \quad (6)$$

$$(\mathrm{RIE})_{B/C} = \left(\sum A_i \gamma_{ij}\right)_{B/C} /K = (1+x)^{2/3}\gamma_{AB} + \gamma_{BC} \quad (7)$$

$$(\mathrm{RIE})_{C/B} = \left(\sum A_i \gamma_{ij}\right)_{C/B} /K = [x^{2/3}\gamma_{BC} + (1+x)^{2/3}\gamma_{AC}] \quad (8)$$

where $K = (4\pi)^{1/3} n_C^{1/3} (3V_C)^{2/3}$ and $(\mathrm{RIE})_{B+C}$ denotes the relative interfacial energy for the separately dispersed morphology of the two minor components, $(\mathrm{RIE})_{B/C}$ for the morphology in which the B-phase encapsulates C, and $(\mathrm{RIE})_{C/B}$ for the morphology in which the C-phase encapsulates B.

Table VII T_{av} and Melt Viscosity (Torque) Ratios at 190°C and 60 rpm

Sample[a]	T_{av} (Nm)[b]	T_{HD}/T_{rubber}[c]	T_{rubber}/T_{PP}	T_{HD}/T_{PP}	T_{av}/T_{PP}
1	17.85	1.16	0.97	1.13	1.05
2	30.2	0.47	2.4	1.13	1.78
3	8.5	0.03	0.97	0.03	0.5
4	20.85	0.01	2.4	0.03	1.23
5	17.25	1.25	0.9	1.13	1.01
6	7.9	0.03	0.9	0.03	0.46

[a] See Table II.
[b] At 50/50 wt % of minor phases.
[c] Rubber phase can be EPR or EPDM.

Viscosity Effect

In a two-phase polymeric blend with disperse-matrix morphology, the viscosity ratio of disperse phase to matrix plays an important role in controlling the size of the dispersed phase.[6,8] However, in ternary blends in which three phases exist, the effect of viscosity on morphology is very complex. Kim et al.[19] reported that for polyolefin ternary blends with core–shell morphology, when two minor phases have the same composition, the minor phase with the lower viscosity encapsulates the one with the higher viscosity.

Luzinov et al.[14] described a core–shell morphology for PS/SBR/PE blends with different melt viscosity ratios of components. These authors assumed that the size of the core is influenced by the viscosity ratio of the core-forming polymer with respect to shell precursor. The viscosity ratio between the matrix and shell phase would then act on the size of the dispersed phase as a whole. Here, this concept was modified and the ratio of average viscosity of two minor phases to matrix was used to predict the size of the dispersed phase. Average viscosity was calculated by means of a simple mixture rule:

$$T_{av} = T_1 x_1 + T_2 x_2 \quad (9)$$

where T is a term related to the viscosity of each phase and x is the volume fraction of individual phases in their core–shell system.

EXPERIMENTAL

Materials

Two types of high-density polyethylene (HDPE), one type of isotactic polypropylene, two types of

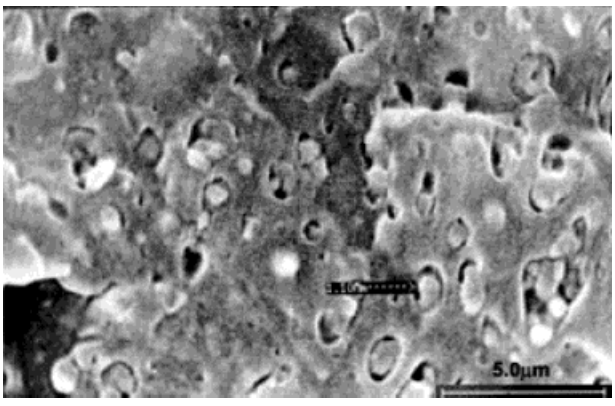

Figure 1 Scanning electron micrograph of PP/EPDM1/HDPE1 blend.

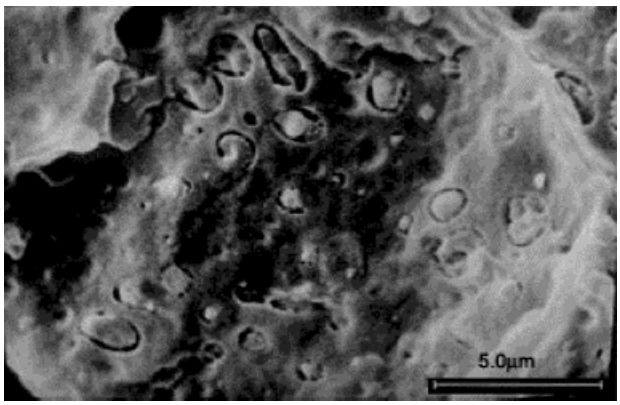

Figure 2 Scanning electron micrograph of PP/EPDM2/HDPE1 blend.

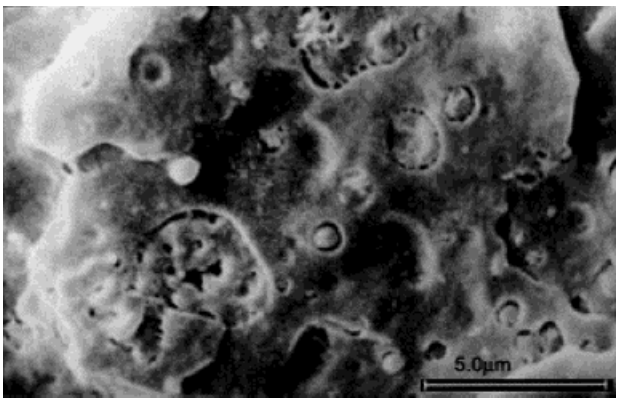

Figure 4 Scanning electron micrograph of PP/EPDM2/HDPE2 blend.

ethylene–propylene–diene terpolymer (EPDM), one type of ethylene–propylene rubber (EPR), and one type of polystyrene (PS) were used for blending .The main properties of these polymers and their producers are listed in Table I.

Blend Preparation

Ternary blends with a 70 wt % composition of the major phase and the two minor phases, each with a 15 wt % composition, were prepared by melt mixing in a Brabender internal mixer equipped with roller-type blades at 190°C and 60 rpm. Nomenclature and components of the blends are listed in Table II.

Blending was carried out by first feeding the rubber into the molten PP and after 3 min mixing, PS or PE was charged into the mixer and mixing was continued for an additional 3 min, after which the mixture was discharged.

Morphology Studies

Morphologies of the blends were studied using scanning electron microscopy (SEM S360; Cambridge Instruments, Worcester, MA). SEM micrographs were taken from cryogenically fractured surfaces of blend specimens. The fracture surfaces of the PP/rubber/PE ternary blends were etched for 24 h at room temperature by cyclohexane, to remove the rubber phase, and then the surfaces were coated with gold before viewing.

RESULTS AND DISCUSSION

Interfacial Tensions

Surface tensions of PP, PE, and PS at 190°C were calculated on the basis of data reported for surface tensions (γ) at 180°C, variation of surface

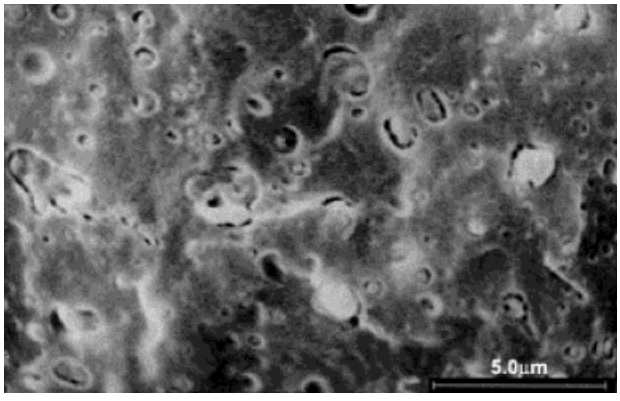

Figure 3 Scanning electron micrograph of PP/EPDM1/HDPE2 blend.

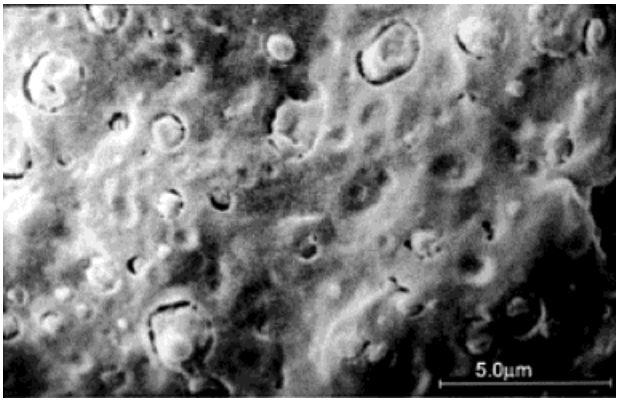

Figure 5 Scanning electron micrograph of PP/EPR/HDPE1 blend.

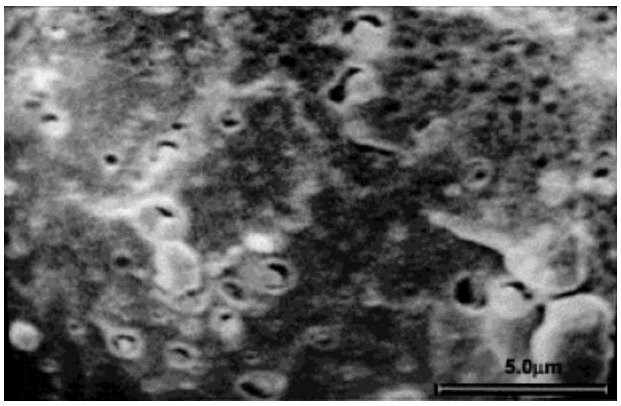

Figure 6 Scanning electron micrograph of PP/EPR/HDPE2 blend.

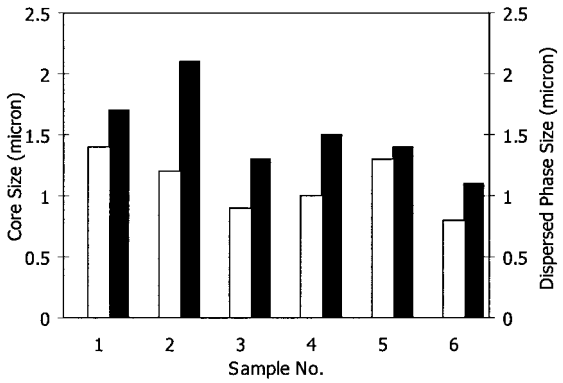

Figure 7 Number-average diameter of PE cores and dispersed phase (micron). □, average diameter of cores (micron); ■, average diameter of dispersed phase (micron).

tensions with temperature ($-d\gamma/dt$), and polarities ($x_p = \gamma_p/\gamma$).[20] Surface tension of EPDM was calculated by means of a simple mixture rule from surface tensions of polyethylidene norbornene (PENB), PE, and PP. The surface tension of PENB was assumed to be the same as that for polybutadiene[14] because the ENB content in EPDM1 and EPDM2 is low (approximately up to 5 wt %). Surface tension γ, dispersive contribution of γ (γ_d), and polar contribution of γ (γ_p) at 190°C for all polymers are listed in Table III.

Interfacial tension between polymers can be calculated from the well-known harmonic mean equation[20] as

$$\gamma_{12} = \gamma_1 + \gamma_2 - \frac{4\gamma_{1d}\gamma_{2d}}{\gamma_{1d} + \gamma_{2d}} - \frac{4\gamma_{1p}\gamma_{2p}}{\gamma_{1p} + \gamma_{2p}} \quad (10)$$

The interfacial tensions calculated from the surface tension data at 190°C are listed in Table IV.

Morphology

PP/EPDM/PE and PP/EPR/PE Ternary Blends

To correlate the phase morphology and the interfacial interaction between components, spreading coefficients and relative interfacial energies (RIE) were calculated from eqs. (1), (2), and (6)–(8). The calculated results are shown in Table V. These results indicate that for all of the ternary blends, λ_{CB} is negative, λ_{BC} is positive, and the morphology in which the B-phase encapsulates the C-phase (B/C) has the lowest value of relative interfacial energy (RIE). Therefore these results predict that for PP/rubber/PE blends the PE phase will be encapsulated by the rubber phase (EPDM or EPR). The steady-state torque obtained from the Brabender mixer (at given temperature and rotor speed) for each component was used as a measure of viscosity, to study the effect of melt viscosity ratios on the morphology of the blends (Table VI). The results of average steady-state torque (T_{av}) of minor components (50/50 vol %) calculated from eq. (9) at 190°C and 60 rpm are listed in Table VII.

Figures 1–6 show SEM micrographs of samples 1–6, respectively. As can be seen, in all of the blends HDPE is encapsulated (completely or partially) by the rubber phase. This is in agreement with the theoretical prediction based on spread-

Table VIII Calculated Spreading Coefficients and Relative Interfacial Energies at 190°C (Samples 7 to 9)

	Blend Components			RIE				
Sample	A	B	C	B/C	C/B	B + C	λ_{BC}	λ_{CB}
7	PP	EPDM1	PS	10.65	4.7	4.38	−0.46	−7.94
8	PP	EPDM2	PS	10.85	5.41	4.69	−0.98	−7.84
9	PP	EPR	PS	10.95	5.56	4.73	−1.11	−7.88

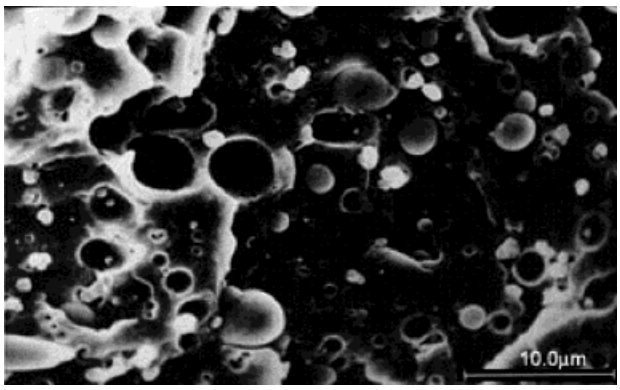

Figure 8 Scanning electron micrograph of PP/EPDM1/PS blend.

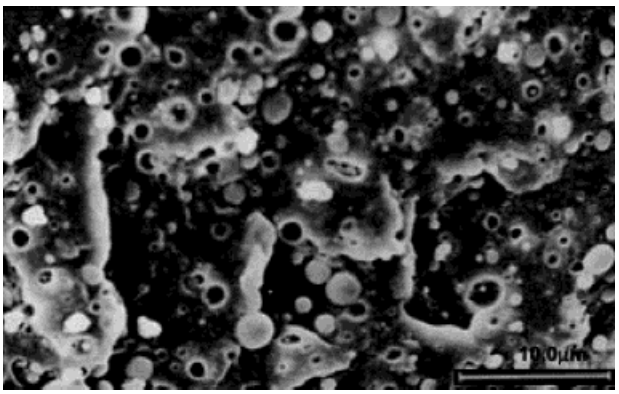

Figure 9 Scanning electron micrograph of PP/EPDM2/PS blend.

ing coefficients and relative interfacial energy data given in Table V. However, from the prediction (Kim et al.[19]) based on the viscosity ratios (T_{HD}/T_{rubber} in Table VII), it is expected that only in samples 1 and 5 rubber forms the shell, whereas in other samples, rubber will be encapsulated by PE. This suggests that for these blends the spreading coefficient and relative interfacial energy play roles in controlling the morphology that are more significant than that of viscosity of components.

The number-average diameters of the PE core and dispersed phase obtained by image analysis for these blends (samples 1–6) are shown in Figure 7. Torque ratio data given in Table VII were used to predict variations in the core size and size of dispersed phase as a whole, in terms of T_{PE}/T_{rubber} and T_{av}/T_{PP}, respectively. From a comparison made between the results of image analysis and torque ratio of components, it was found that for PP/EPDM/PE ternary blends, the number-average diameter of the dispersed phase increased from 1.3 to 2.1 μm, when the ratio of average torque to PP torque (T_{av}/T_{PP}) increased from 0.5 to 1.78. In addition the number-average diameter of the PE core increased from 1.0 to 1.4 μm with increasing T_{HD}/T_{EPDM} from 0.01 to 0.16 (samples 1–4 in Fig. 7).

According to the prediction of Luzinov et al.[14], in a ternary blend with core–shell morphology the number-average diameter of the dispersed phase increases with increasing torque ratio of shell component to matrix (T_{EPDM}/T_{PP}). It is therefore expected that the number-average diameter of the dispersed phase in sample 1 is equal to that of sample 3 and the number-average diameter of sample 2 is equal to that of sample 4. This was not found to be in agreement with our experimental results. Our experimental results as well as our predictions suggest that for ternary blends with core and shell morphology, the ratio of average viscosity of two minor phases to matrix (T_{av}/T_{matrix}) is a more effective parameter than the viscosity ratio of shell component to matrix (T_{shell}/T_{matrix}) in determining the dispersed phase size.

In PP/EPR/PE ternary blends, indicated as samples 5 and 6, sample 5 has a lower dispersed phase size (with lower T_{av}/T_{PP}) and also a lower core size (with a lower T_{HD}/T_{PP}) than that of sample 6.

PP/EPDM/PS and PP/EPR/PS Ternary Blends

Spreading coefficients and relative interfacial energies of samples 7–9 at 190°C calculated from eqs. (1), (2), and (6)–(8) are listed in Table VIII.

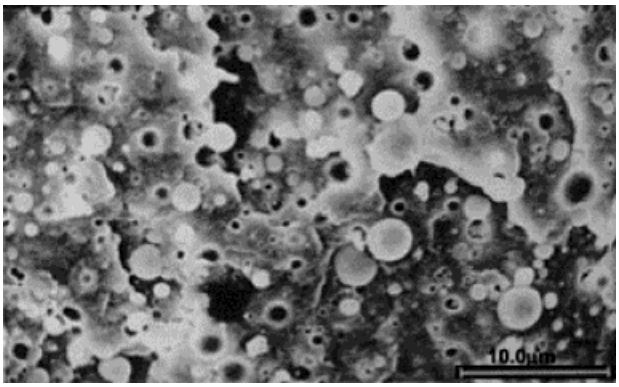

Figure 10 Scanning electron micrograph of PP/EPR/PS blend.

The calculated results indicate that for these blends, λ_{BC} and λ_{CB} are negative and the morphology in which the PS and rubber phases form two distinct phases separately dispersed in the PP matrix (B + C morpholgy) has the lowest value of relative interfacial energy (RIE). SEM micrographs of samples 7–9 are shown in Figures 8–10, from which it can be seen that in these samples the rubber and PS phases disperse separately in the PP matrix. The appearance of the PS particles was found to be different from that of the rubber particles. The rubber particles have irregular shapes, whereas the PS particles are more spherical with a smooth surface.

A comparison made between these results and those predicted on the basis of spreading coefficients and relative interfacial energies given in Table VIII shows that there is a good agreement between experimental and theoretical results.

For this type of morphology the torque ratios of each dispersed phase to PP can be used to predict the average particle size of dispersed phases. The calculated results are given in Table IX.

The number-average diameters of each phase measured by image analysis are given in Table X. As expected from the calculated results given in Table IX, the PS particle size remains almost the same in samples 7–9, whereas the rubber particle size varies in these three samples. Considering the data of T_{rubber}/T_{PP}, it is expected that the size of the rubber phase in sample 9 would be lower than that of the other two samples, which is not in accordance with image analysis results (Table X). The reason for this is that the interfacial tension between EPR and PP in sample 9 is higher than that between EPDM1 and PP in sample 7 (Table IV) and thus the rubber phase in sample 7 has a minimum size. For samples 8 and 9 the interfacial tension between rubber and PP is almost the same (Table IV); thus it is expected that sample 9 with lower T_{rubber}/T_{PP} has smaller rubber particles. Thus the image analysis results are in accordance with the prediction based on the torque ratio and interfacial tension data given in Tables IV and IX.

Table IX Torque Ratios of Components at 190°C

Sample	T_{PS}/T_{PP}[a]	T_{Rubber}/T_{PP}
7	1.93	0.97
8	1.93	2.4
9	1.93	0.9

[a] T_{PS} = 32.1 N/m from Table VI.

Table X Number-Average Diameter of Rubber and PS in PP

	Number-Average Diameter (μm)	
Sample	Rubber Phase	PS Phase
7	1.1	2.8
8	1.8	3
9	1.4	2.6

CONCLUSIONS

PP/rubber/PE ternary blends showed a core–shell morphology in which the PE core is encapsulated by the rubber shell. In PP/rubber/PS ternary blends, the two minor phases remain dispersed separately in the PP matrix.

Models based on the interfacial free energy and spreading coefficient predict almost the same morphology for each ternary system. Melt viscosity ratio of components has no appreciable influence on the type of morphology and can affect the size of only dispersed phases, at least with the mode of preparation used.

The results showed that interfacial interaction between phases is a major parameter that controls the phase structure in ternary polymer blends.

The size of dispersed phases for all blends can be related to the torque ratios of components.

REFERENCES

1. Xanthos, M. Polym Eng Sci 1988, 28, 1392.
2. Utracki, L. A. Int Polym Sci Technol 1991, 18, T38.
3. Utracki, L. A. Commercial Polymer Blends, 1st ed.; Chapman & Hall: London, 1998; Chapters I–III.
4. Favis, B. D.; Chalifoux, J. P. Polymer 1988, 29, 1761.
5. Favis, B. D. J Appl Polym Sci 1990, 39, 283.
6. Favis, B. D.; Chalifoux, J. P. Polym Eng Sci 1987, 27, 1591.
7. Willis, J. M.; Favis, B. D. Polym Sci 1990, 28, 2259.
8. Wu, S. Polym Eng Sci 1987, 27, 335.

9. Elmendorp, J. J.; Vandervegt, A. K. Polym Eng Sci 1986, 26, 1332.
10. Kojima, T.; Kikuchi, Y.; Inoue, T. Polym Eng Sci 1992, 32, 1863.
11. Gupta, A. K.; Srinivasan, K. R. J Appl Polym Sci 1993, 47, 167.
12. Guo, H. F.; Packirisamy, S.; Gvozdic, N. V.; Meier, D. J. Polymer 1997, 38, 785.
13. Tjong, S. C.; Li, W. D.; Li, R. K. Y. Eur Polym J 1998, 34, 755.
14. Luzinov, I.; Pagnoulle, C.; Xi, K.; Huynh-Ba, G.; Jerome, R. Polymer 1999, 40, 2511.
15. Gupta, A. K.; Jain, A. K.; Ratnam, B. K.; Maiti, S. N. J Appl Polym Sci 1990, 39, 515.
16. Zheng, W.; Leng, Y.; Zhu, X. Plast Rubber Compos Process Appl 1996, 25, 490.
17. Hobbs, S. Y.; Dekkers, M. E.; Watkins, V. H. Polymer 1988, 29, 1598.
18. Harkins, W. D. The Physical Chemistry of Surface Films; Reinhold: New York, 1952; p. 23.
19. Kim, B. K.; Kim, M. S.; Kim, K. J. J Appl Polym Sci 1993, 48, 1271.
20. Wu, S. Polymer Interface and Adhesion; Marcel Dekker: New York, 1982.